Analysis of Prepeak Structure of Concentrated Organic Lithium Electrolyte by Means of Neutron Diffraction with Isotopic Substitution and Molecular Dynamics Simulation

Journal:	*The Journal of Physical Chemistry*
Manuscript ID	jp-2017-00686e.R3
Manuscript Type:	Article
Date Submitted by the Author:	08-May-2017
Complete List of Authors:	Yamaguchi, Tsuyoshi; Nagoya Daigaku Kogakubu Daigakuin Kogaku Kenkyuka, Department of Molecular Design and Engineering Yoshida, Koji; Fukuoka University, Chemistry Yamaguchi, Toshio; Faculty of Science, Dept. of Chemistry Kameda, Yasuo; Faculty of Science, Yamagata University, Dept. of Material & Biological Chemistry Ikeda, Kazutaka; High Energy Accelerator Research Organization (KEK), Institute of Materials Structure Science Otomo, Toshiya; High Energy Accelerator Research Organization, Institute of Materials Structure Science

Analysis of Prepeak Structure of Concentrated Organic Lithium Electrolyte by Means of Neutron Diffraction with Isotopic Substitution and Molecular Dynamics Simulation

Tsuyoshi Yamaguchi,[a,*] *Koji Yoshida,*[b] *Toshio Yamaguchi,*[b] *Yasuo Kameda,*[c] *Kazutaka Ikeda,*[d] *and Toshiya Otomo*[d]

[a] Department of Molecular Design and Engineering, Graduate School of Engineering, Nagoya University, Furo-cho, Chikusa, Nagoya, Aichi 464-8603, Japan

[b] Department of Chemistry, Faculty of Science, Fukuoka University, Nanakuma, Jonan, Fukuoka 814-0180, Japan

[c] Department of Material and Biological Chemistry, Faculty of Science, Yamagata University, 1-4-12, Kojirakawa-machi, Yamagata City, Yamagata 990-8560, Japan

[d] High Energy Accelerator Research Organization (KEK), Tsukuba, Ibaraki 305-0801, Japan

E-mail: tyama@nuce.nagoya-u.ac.jp (T. Yamaguchi)

CORRESPONDING AUTHOR: E-mail: tyama@nuce.nagoya-u.ac.jp, Tel: +81-52-789-3592, Fax: +81-52-789-3273.

Abstract

The prepeak structure of a 3 mol / kg solution of $LiClO_4$ in propylene carbonate (PC) was studied by both neutron diffraction with isotopic substitution (NDIS) and molecular dynamics (MD) simulation. The NDIS data showed that the intensity of the prepeak decreases experimentally with increasing the scattering length of the lithium atom from ^{7}Li to ^{6}Li in PC-d_6. On the other hand, although the prepeak was observed in solutions of both PC-d_6 and PC-h_6, it disappears when the 1:1 mixture of PC-d_6 and PC-h_6 was used as the solvent. The prepeak structure and its variation with the isotope substitution were reproduced well by MD simulation, and they were explained in terms of the contrast of the scattering length densities of the ionic and nonpolar domains.

1. Introduction

Physicochemical properties of concentrated organic electrolyte solutions have been drawing considerable attention for recent years. It has been demonstrated that the electrolysis of solvents is suppressed in concentrated lithium electrolytes, so that these electrolyte solutions have potential application to high-voltage lithium ion batteries.[1,2,3] In addition, "deep eutectic solvents" composed of salts and neutral organic molecules have been studied as low-cost alternatives of room temperature ionic liquids.[4,5,6] In order to understand the physicochemical properties of the concentrated organic electrolyte solutions from the molecular view points, the information of their liquid structures is indispensable.

The liquid structure in the reciprocal space can be probed by diffraction experiments using quantum beams such as X-rays or neutron. In particular, the neutron diffraction experiment has an advantage that the structure associated with a particular atom can be probed in a selective way through the isotope substitution method. The neutron diffraction with isotope substitution (NDIS) method has been applied to some concentrated electrolyte solutions containing lithium atoms.[7,8,9]

The structure factor of liquids determined by diffraction experiments usually exhibits a strong peak at a wavenumber corresponding to the reciprocal length of the intermolecular contact distance, which is hereafter called "main peak". Some liquids show an additional peak at the wavenumber lower than that of the main peak, which is called "prepeak". The prepeak indicates the presence of a mesoscopic structure whose spatial dimension is larger than the intermolecular contact distance.

A famous example of the prepeak structure is that of molten silica, which is assigned to its characteristic tetrahedral network structure.[10] The prepeak structure of room-temperature ionic liquids has been attracting many researchers for a decade, and it is now clarified that the prepeak of ionic liquids originates in the mesoscopic structure composed of polar and nonpolar domains.[11,12,13,14,15] Another class of liquids that shows the prepeak structure is higher alcohols with long alkyl chain.[16,17,18] Very recently, Perera demonstrated that the prepeaks of room-temperature ionic liquids and higher alcohols have a similar origin.[19] Some studies reported the prepeak in the structure factor of concentrated organic

electrolyte solutions.[20,21,22] In the case of the organic electrolytes, however, it is not clarified yet whether the origin of the prepeak is the same as that of room-temperature ionic liquids.

We recently performed a quasi-elastic neutron scattering experiment on the concentrated solution of $LiPF_6$ in propylene carbonate (PC).[23] The static structure factor of the solution shows a prepeak around 0.8 $Å^{-1}$ when the concentration of the salt is not lower than 2 mol / kg, in addition to the main peak at 1.4 $Å^{-1}$ which is visible at all the concentrations. The intermediate scattering function was measured at both the prepeak and the main peak. The relaxation at the prepeak is several times slower than that at the main peak. Comparing with the frequency-dependent transport properties, such as the shear viscosity and the electric conductivity, the role of the dynamics at the main peak is dominant in shear viscosity, while a possible role of the prepeak dynamics in the ionic conductivity was suggested.[23] However, further discussion was not possible at that time because of the lack of the origin of the prepeak.

In this work, the prepeak structure of 3 mol / kg $LiClO_4$ / PC solution was investigated by means of NDIS and molecular dynamics (MD) simulation. The isotope substitution was performed both on ^6Li / ^7Li and H / D pairs, and the variation of the height of the prepeak with the isotope substitutions was analyzed. The anion was changed from PF_6^- to ClO_4^- in order to avoid the hydrolysis of the anion during the anion exchange reaction for the preparation of the isotope-substituted lithium salts. The prepeak structure of $LiClO_4$ / PC solution was similar to that of $LiPF_6$ / PC one, as will be shown later in this paper. We consider that the molecular picture of the prepeak obtained in this work on the former also applies to the latter. With confirming that the MD simulation can reproduce the prepeak and the effects of the isotope substitution well, the molecular origin of the prepeak is extracted from the MD simulation.

2. Theoretical Background

The total static structure factor of liquids obtained by the neutron diffraction experiment, denoted as $I_n(q)$, is given by the linear combination of the partial structure factor, $\chi_{ij}(q)$, as

$$I_n(q) = \sum_{ij} b_i b_j \chi_{ij}(q), \tag{1}$$

where the wavenumber q is given as $4\pi\sin\theta/\lambda$ with the scattering angle 2θ and the wavelength λ, and b_i stands for the coherent scattering length of the atom i. The partial structure factor is defined as[24]

$$\chi_{ij}(|q|) \equiv \frac{1}{V}\left\langle \rho_i^*(\mathbf{q})\rho_j(\mathbf{q})\right\rangle. \tag{2}$$

Here, $\rho_i(\mathbf{q})$ denote the density field of atom i in the reciprocal space, and V means the volume of the system. It is to be noted here that the prefactor at the rhs. depends on literatures.

Provided that the Hamiltonian of the classical system is described as the sum of the kinetic and potential parts, the spatial correlation between atoms does not depend on the kinetic parameters. It is thus a good approximation that $\chi_{ij}(q)$ does not change with isotope substitution. On the other hand, the coherent scattering length b_i does change on isotope substitution. For example, the coherent scattering lengths of ^{6}Li and ^{7}Li atoms are b_6 = +2.00 fm and b_7 = -2.22 fm, respectively, and those of H and D atoms are b_H = -3.741 fm and b_D = +6.671 fm, respectively.[25] Therefore, the information on $\chi_{ij}(q)$ associated with the element i can be extracted from the comparison between $I_n(q)$s of different isotopes of the element i.

In this work, we performed the diffraction experiments on the samples containing mixtures of isotopes, of which special cares must be taken. The story is simple in the case of the mixtures of ^{6}Li and ^{7}Li, where eq. (1) is modified to give the total scattering profile as

$$I_n(q) = \sum_{ij} \bar{b}_i \bar{b}_j \chi_{ij}(q) + x_6 x_7 (b_6 - b_7)^2, \tag{3}$$

$$\bar{b}_i = \begin{cases} x_6 b_6 + x_7 b_7 & (i = \mathrm{Li}) \\ 0 & (\mathrm{otherwise}) \end{cases}, \tag{4}$$

where x_6 and x_7 stand for the mole fraction of ^{6}Li and ^{7}Li, respectively. Since the second term of the rhs. of eq. (3) behaves as the constant background, the observed structure factor is essentially realized as that of the single-isotope sample for which the coherent scattering length of the Li atom is given by the average value of ^{6}Li and ^{7}Li defined as eq. (4). The Cl-atom in ClO_4^-, which consists of ^{35}Cl and ^{37}Cl in

samples of the natural isotope abundance, can be treated in a similar way because the ClO_4^- ion contains only a single Cl-atom, and the Cl-atom of natural isotope mixture can also be regarded as the single-isotope sample of the average coherent scattering length.

The situation is more complicated when we use the mixture of PC-h_6 and PC-d_6, because proton exchange reaction does not occur between PC-h_6 and PC-d_6. The correlation between H and D atoms appear in the intermolecular cross correlation, while it is absent in the *intramolecular* one. In such a case, eq. (1) is modified and the total scattering profile is given by[26]

$$I_n(q) = \sum_{ij} \overline{b}_i \overline{b}_j \chi_{ij}(q) + x_H x_D \sum_{ij} \delta b_i \delta b_j \left[\boldsymbol{\rho} \cdot \boldsymbol{\omega}(q)\right]_{ij}, \tag{5}$$

$$\overline{b}_i = \begin{cases} x_H b_H + x_D b_D & (i \in \text{Hydrogen}) \\ 0 & (\text{otherwise}) \end{cases}, \tag{6}$$

$$\delta b_i = \begin{cases} b_H - b_D & (i \in \text{Hydrogen}) \\ 0 & (\text{otherwise}) \end{cases}, \tag{7}$$

where x_H and x_D stand for the mole fraction of H and D atoms, respectively. The second term of the rhs. of eq. (5) is now dependent on q. It is described in terms of the intramolecular correlation function defined as

$$\left[\boldsymbol{\rho} \cdot \boldsymbol{\omega}(|q|)\right]_{ij} \equiv \frac{1}{V} \left\langle \rho_i^*(\mathbf{q}) \rho_j(\mathbf{q}) \right\rangle_s, \tag{8}$$

where the suffix '*s*' indicates that only the correlation between two atoms in the same molecule is taken into account.

Equation (5) is a famous equation in the small-angle neutron scattering (SANS) spectroscopy of polymers, and the use of isotopic mixtures is a well-established tool to determine the single-chain conformation of concentrated polymer systems.[26] The intramolecular term, [$\boldsymbol{\rho}\cdot\boldsymbol{\omega}(q)$] of the rhs. of eq. (5), exhibits a peak at q = 0, and the width of the peak represents the size of a molecule. It is to be noted here that the intramolecular term appears solely in the case of isotopic mixtures, and that it disappears in isotopically pure samples, because $x_D = 0$ or $x_H = 0$.

3. Experimental

3.1. Materials

Deuterated propylene carbonate (PC-d_6), $C_4D_6O_3$ (> 98 atom% D, Battery grade) was purchased from Wako and used as received. Propylene carbonate (PC-h_6, Lithium battery grade) was purchased from Kishida and dried over molecular sieves 3A prior to use. PC-m_6 was prepared by mixing the PC-d_6 with PC-h_6 with the same mole ratio. $HClO_4$ (Kanto Chemicals, 60%) was then reacted with aqueous solutions of $^6Li_2CO_3$ and $^7Li_2CO_3$ (Tomiyama High Purity Chemicals, ^6Li > 95.4 % and ^7Li > 99.96 %, respectively) to prepare aqueous solutions of $^6LiClO_4$ and $^7LiClO_4$, respectively. After successive evaporation of water, the isotopically labelled $LiClO_4$ powders were finally dried under vacuum at 393 K for 24 h. $^0LiClO_4$ was prepared by mixing the $^6LiClO_4$ with $^7LiClO_4$ with the ratio (^6Li : ^7Li = 44.9 : 55.1), so that the average coherent scattering length of lithium is equal to zero. The sample solutions were prepared by direct dissolution of $^6LiClO_4$ and $^7LiClO_4$, respectively, into PC to a required amount. The molar ratios of $LiClO_4$ to PC of all the solutions were fixed to that of the $LiClO_4$ / PC solution at 3 mol / kg with the natural isotope abundances. The densities of the sample solutions were calculated from that of the 3 mol / kg solution with natural isotope abundances[23] under the assumption that the molar volume of the solution does not change upon the isotope substitution. The parameters of the sample solutions were listed in Table 1. The first three are the series of the isotope substitution of Li, while the second, fourth and fifth are that of hydrogen.

Table 1. Average coherent scattering lengths of lithium, $\bar{b}_{Li}$, and hydrogen, $\bar{b}_H$, the number density of PC, ρ_0, incoherent scattering cross section, σ_i, and absorption cross section, σ_a, at 1 Å of the samples.

The isotopic purities of ^{6}Li, ^{7}Li, H and D were assumed to be 100 %, because the exact amounts of the isotopic impurities were not determined.

	$\bar{b}_{Li}$ / 10^{-15} m	$\bar{b}_{H}$ / 10^{-15} m	ρ_0 /Å^{-3}	σ_i/ barns	σ_a / barns
^{6}LiClO$_4$/PC-d_6	2.00	6.671	0.09110	0.9342	11.00
^{7}LiClO$_4$/ PC-d_6	-2.22	6.671	0.09110	0.9407	0.3796
^{0}LiClO$_4$/ PC-d_6	0.0027	6.671	0.09110	0.9372	5.972
^{7}LiClO$_4$/ PC-h_6	-2.22	-3.739	0.09110	32.10	0.4531
^{7}LiClO$_4$/ PC-m_6	-2.22	1.473	0.09110	16.50	0.4163

3.2. Neutron diffraction

Neutron diffraction experiment was performed at 298 K on the High Intensity Total Diffractometer (NOVA) installed at the beamline BL21 of Materials and Life Science Experimental Facility (MLF) in Japan Proton Accelerator Research Complex (J-PARC). The incident neutron beam was generated by the proton accelerator whose output power was 300 kW. Scattered neutrons were detected by ^{3}He position sensitive counter at 20° (13.1 − 27.9°). The beam height was 20 mm. The sample solutions were put into a flat null V-Ni alloy of the wall thickness of 0.1 mm with sample thickness of 2 mm, width of 10 mm, and height of 50 mm. The sample cans were placed in a vacuum chamber. A vanadium plate of 1.5 mm was measured to normalize the experimental intensity to absolute units. An empty cell and background were also measured. The data accumulation time was 3-11 hr. The data measured were corrected for background, absorption,[27] and multiple scattering[28] in the sample and the cell, and then normalized to absolute units by use of the data for the vanadium plate. These corrections were performed with nvaSq program.[29] The neutron scattering lengths and cross sections were referred to the web site of NIST center.[25] Finally, 10 total scattering functions $S(Q)$ data in the range of 13.1–27.9° of scattering angle for 20 detector bank without inelasticity (Placzek) correction.

The inelasticity effect would be proportional to the reciprocal of atomic mass.[30] Hence, hydrogen atom in the systems mainly gives a distortion in the structure function. The inelasticity correction was made in the manner developed by Kameda et al.[31] That is, the self-scattering intensity observed for the null-H_2O was subtracted from the $S(Q)$ of sample solutions. The subtraction factors were determined so that all $S(Q)$s were overlapped. The details were described in the Supporting Information.

4. MD simulation

We performed MD simulation on systems containing 158 PC molecules and 49 $LiClO_4$ ion pairs, which correspond to the concentration of 3.04 mol / kg. The PC was the equimolar racemic mixture. The simulation runs were performed under the *NVT* ensemble, in order to avoid the fluctuation of the lattice vectors during the calculation of the structure factor in the reciprocal space. The solution was enclosed in a cubic cell, whose size was determined to be 2.949 nm to reproduce the mass density at 3 mol / kg at room temperature.[23] The comparison with experiments was performed at the same density because molecular packing plays a crucial role in determining the microscopic structure of dense liquids.[24]

Both PC and ClO_4^- were described by all-atom models. The interaction parameters for PC were taken from those proposed by You and coworkers,[32] with which they have reproduced the dielectric properties of liquids well. Three different models were employed for $LiClO_4$ in order to investigate the effects of the strength of the ion association on the prepeak structure. In Model 1, the parameters of Li^+ were taken from Soetens and coworkers,[33] while those for ClO_4^- was from Heinje and coworkers.[34] Although the bond lengths and the bond angles were fixed in the original model of Heinje and coworkers, we treated them as flexible, and the intramolecular potential parameters were taken from those proposed by Cadena and Maginn.[35] In Model 2, the Li^+ ion was the same as that of Model 1, and the ClO_4^- ion was taken from that proposed by Kasahara and Sato,[36] except that the parameters for intramolecular bonds

were taken from Cadena and Maginn.[35] In Model 3, the Li^+ ion was taken from Jensen and Jorgensen,[37] while ClO_4^- ion was from Cadena and Maginn.[35] The most important difference among the three models is the partial charge on the O-atoms of ClO_4^-, which are -0.3590*e*, -0.5203*e* and -0.5855*e* in Models 1, 2 and 3, respectively. The ion association between Li^+ and ClO_4^- is thus the weakest in Model 1 and the strongest in Model 3.

The partial structure factors, $\chi_{ij}(q)$, were evaluated directly in the reciprocal space according to the definition given by eq. (2). The calculation of the intramolecular correlation function, $\omega_{ij}(q)$ was performed also in the reciprocal space according to eq. (8). The masses of the H- and Li-atoms were fixed to be the values determined from the natural isotope abundances in all the runs, and $I_n(q)$ for various isotope combinations were calculated solely by changing the scattering lengths. The coherent scattering lengths of all the nuclei were taken from the web page of the NIST Center for Neutron Research, National Institute of Standards and Technology.[25]

The MD simulations were performed using GROMACS 5.1.2 package.[38] The .itp file for PC was taken from the literature.[32] The equation of motion was integrated by the leap-frog algorithm with the time step of 1 fs. The spatial coordinates of all the atoms were recorded at every 1 ps for the calculation of the static structure factor. The temperature of the system was controlled by the Nosé-Hoover method.[39] The particle-mesh-Ewald method was employed for the long-range part of the Coulombic interaction, and the size of the Fourier spacing was 0.12 nm. The bond lengths associated with the H-atoms were fixed with LINCS algorithm.[40] The snapshot was drawn using VMD software.[41]

The temperature of the system was fixed to be 500 K for all the models. Although we tried runs at room temperature, the relaxation was extremely slow and we could not obtain the converged static structure factor. The production runs of the three models were 10 ns length, proceeded by the equilibration runs of 10 ns length. As will be shown in the next section, only Model 1 can reproduce the prepeak structure. We therefore performed an additional run of 100 ns length on Model 1 to improve the statistical qualities of the correlation functions. The simulation run of Model 1 at 350 K was also performed, whose lengths of the equilibration and the production runs were 20 ns and 100 ns,

respectively. The temperature dependence of the static structure factor was rather small, as is demonstrated in Fig. S1 of Supporting Information, and we consider that the structure obtained by the MD simulation at 500 K captures the essential feature of the static structure factor determined by the experiment at 298 K. The intermediate scattering functions at both prepeak and the main peak were calculated at 500 K with Model 1, although the results are not exhibited for brevity. It was confirmed that the length of the equilibration runs, 10 ns, is sufficiently long compared with the structural relaxation times.

5. Results and Discussion

5.1. NDIS experiment

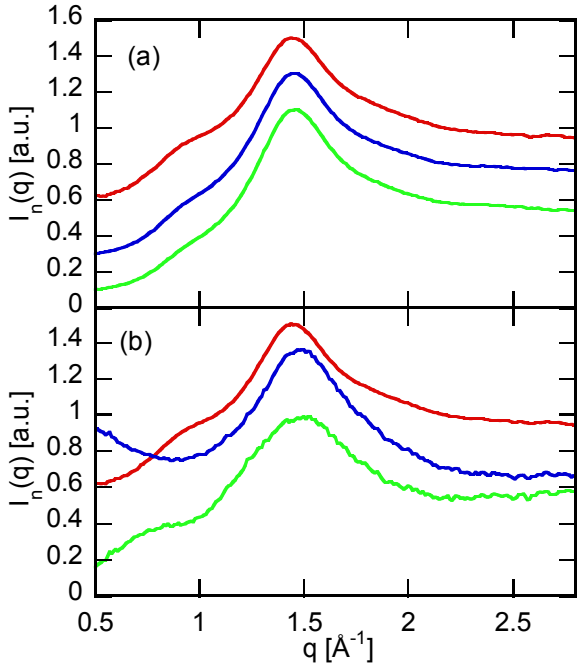

Figure 1. The static structure factors of $LiClO_4$ / PC solutions determined by the neutron diffraction experiments, $I_n(q)$, are shown as a function of wavenumber, q. In panel (a), the isotope composition of the Li-atom is changed as ^{7}Li (red), ^{0}Li (blue), and ^{6}Li (green), while the solvent was fixed to be PC-d_6.

In panel (b), $^{7}LiClO_4$ is dissolved into PC-d_6 (red), PC-m_6 (blue), and PC-h_6 (green). The structure factors in both panels are scaled and shifted to improve the visibility.

Figure 1 shows the static structure factors obtained by the neutron experiment. The total scattering profiles are plotted in Fig. 1, rather than extracting the partial correlation functions associated with the lithium or hydrogen atoms. The effects of the isotope substitutions of the lithium and hydrogen atoms are exhibited in Figs. 1a and 1b, respectively. The prepeak appears around q = 0.8 Å^{-1} in $^{7}LiClO_4$ / PC-d_6 solution, as we have reported on $^{7}LiPF_6$ / PC-d_6 solution.[23]

The height of the prepeak decreases gradually from ^{7}Li to ^{6}Li, as is shown in Fig. 1a. Given that the coherent scattering lengths of ^{7}Li and ^{6}Li are -2.22 fm and +2.00 fm, respectively,[25] the height of the prepeak is a decreasing function of the scattering length of the Li atom.

The variation of the structure factor in the low-q region is more drastic in the series of the isotope substitution of the hydrogen atom. The prepeak is observed in both PC-d_6 and PC-h_6 solutions, and its peak position is shifted slightly to the lower-q in the latter. In PC-m_6, however, the prepeak is absent in the same wavenumber region, and the increase in the scattering strength is observed at the lower wavenumber.

5.2. MD simulation

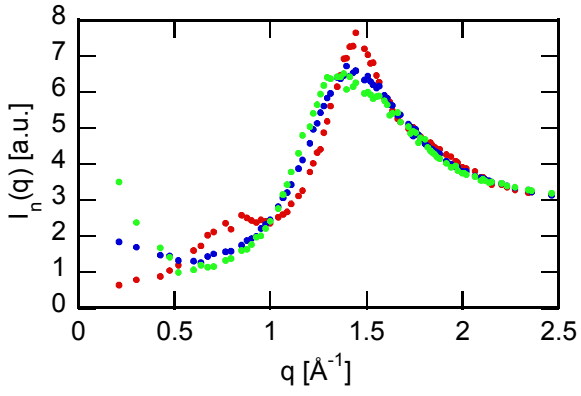

Figure 2. The static structure factor of $^{7}LiClO_4$ / PC-d_6 using Models 1 (red), 2 (blue) and 3 (green).

The static structure factors of $^{7}LiClO_4$ / PC-d_6 were calculated for the three models with the simulation runs of 10 ns lengths, and the results are shown in Fig. 2. The structure factor in the low-q region (q < 1 Å^{-1}) is strongly model-dependent. Model 1 reproduces the prepeak at 0.8 Å^{-1} as is observed experimentally in Fig. 1. On the other hand, the prepeak is not visible in other two models, and the strong scattering is observed at q < 0.5 Å^{-1}. The low-q scattering usually suggests the concentration fluctuation, and the presence of the large aggregation of ions is expected in Models 2 and 3. The strength of the low-q scattering is larger in Model 3 than in Model 2, which is in harmony with the stronger ion association in the former.

The solvation structures of Li^+ are shown in Figs. S2 and S3 of Supporting Information as the radial distribution function and the running coordination number, respectively. The first peak of $g_{LiCl}(r)$ grows from Models 1 to 3 as is expected. The first peak of $g_{LiCl}(r)$ splits into two due to the coexistence of the monodentate and bidentate coordination structures. In addition, the values of $g_{LiCl}(r)$ at r = 4 - 8 Å also increases, suggesting the growth of large ionic aggregates. The coordination number of solvent PC varies in the opposite way, because the solvent PC is excluded from the first solvation shell of Li^+ by the anion.

We hereafter analyze the simulation run of Model 1 that can reproduce the prepeak.

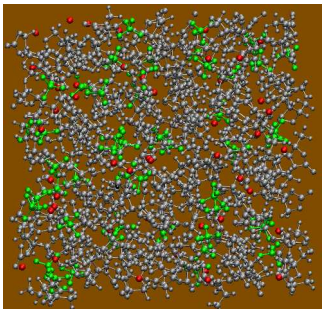

Figure 3. The snapshot of the simulation run of Model 1. The Li^+ cation, ClO_4^- anion, and PC solvent are drawn with red, green, and gray colors, respectively.

The snapshot of the simulation run of Model 1 is demonstrated in Fig. 3. Small chain-like aggregates of ions are observed somewhere, in which the cation and the anion are aligned in an alternating way. The linear aggregates are separated from each other by PC solvents, which coordinate to the Li^+ ion. The chain-like structure of the solution is similar to that Seo and coworkers reported on the mixed crystals of lithium salts and ethylene carbonate.[42] Since the chain-like structure of ions resembles that of higher alcohols, it can be the origin of the prepeak as is observed in higher alcohols.[19]

The coordination number of the Li^+ ion is 4 in our simulation as was reported by Kameda and coworkers on 1 M solutions of lithium salt in PC,[8] and the competition occurs between the anion and the solvent for the coordination to the cation. In Model 1, the average coordination number of the anion is 1.5 as is shown in Fig. S3b, which is in harmony with the short-chain structure of 4 ions on average. The remaining 2.5 coordination is accomplished by PC solvent molecules (Fig. S3a), which keeps the chains apart. The stronger negative charges on the O-atoms in Models 2 and 3 favor the coordination of the anion to that of the solvent, leading to the formation of large ionic aggregates.

The success of Model 1 in reproducing the prepeak does not mean that Model 1 is the best model to describe the solution of $LiClO_4$ / PC under every condition. First, all the potential parameters of solvent PC are same in all the models employed in our present study. Since the suppression of the coordination of the anion to the cation is a result of the competition between the anion and the solvent, it could be achieved by an increase in the partial charge on the carbonyl O-atom of PC. Second, we consider that the success of the model with weak charge on the O-atom of ClO_4^- in the concentrated solution is due to the large polarizability of the anion. The three models of the anion employed in this work are rigid ion models, where the effects of the polarizability of the anion are effectively included in the values of the fixed partial charges on the anion. The term "effectively" indicates that the suitable values of the rigid partial charges may depend on the environment of the anion. When a Li^+ cation approaches a ClO_4^- anion, the polarization of the anion increases the partial charge on the O-atom coordinated to the cation, which is described effectively by the non-polarized model as the large negative rigid charge on all the O-atoms. On an approach of an additional Li^+ cation to another O-atom that is not coordinated to the first

Li^+ cation, however, the effective charge felt by the second cation is smaller than that by the first one due to the polarization induced by the first cation. We consider that the non-polarizable Model 1 effectively describes the non-additive effect of the polarization in the concentrated solution through the weak negative charge on the O-atom. It should be kept in mind, however, that the reduction of the rigid partial charge is a mere effective way to include the effects of the polarization, and the detailed structure described by Model 1, such as the existence of the bidentate coordination, may not correspond to that of real solutions.

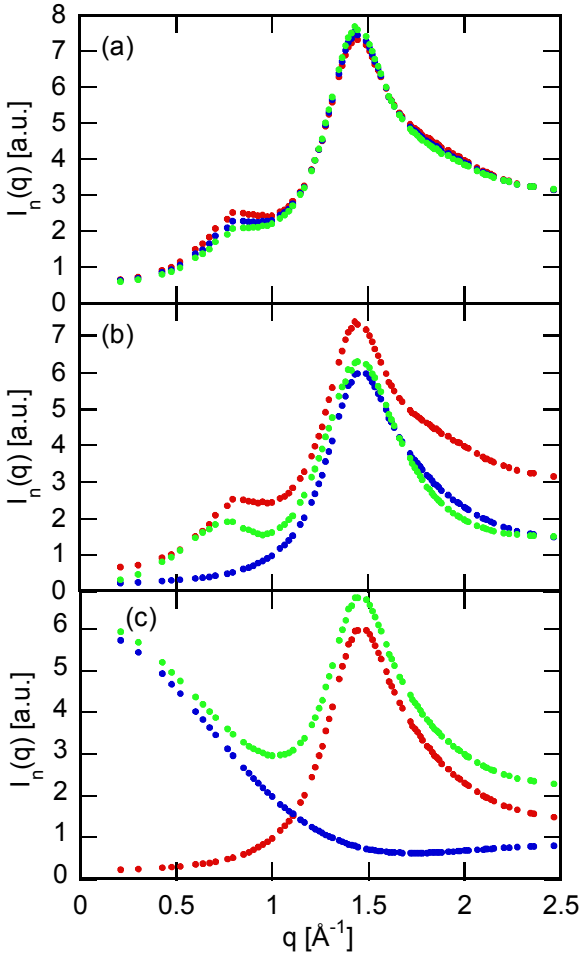

Figure 4. The neutron static structure factors, $I_n(q)$s, of various isotope compositions are plotted. The meanings of the colors in panels (a) and (b) are the same as those in the corresponding panels of Fig. 1. In panel (a), the Li^+ ion is varied as ^{7}Li (red), ^{0}Li (blue) and ^{6}Li (green), keeping the solvent as PC-d_6. In panel (b), the solvent is varied as PC-d_6 (red), PC-m_6 (blue) and PC-h_6 (green), keeping the salt as $^7LiClO_4$. The intramolecular correlations, the second terms of the rhs. of eqs. (3) and (5), are not

included in these panels. In panel (c), the first and the second terms of the rhs. of eq. (5) for $^7LiClO_4$ / PC-m_6 are shown with red and blue symbols, respectively, and the total structure factor is drawn with the green symbol.

The neutron static structure factors of various isotope compositions are calculated using the 100 ns simulation run of Model 1. The result of the isotope substitution of the Li atom in PC-d_6 is shown in Fig. 4a. The constant background due to the self correlation, the second term of the rhs. of eq. (3), is not included here. The prepeak becomes gradually weaker with increasing the scattering length of Li-atom from b_7 = -2.22 fm to b_6 = +2.00 fm, as is observed experimentally in Fig. 1a.

The effect of the isotope substitution of the hydrogen atom of $^7LiClO_4$ / PC is exhibited in Fig. 4b. The additional term due to the intramolecular correlation, the second term of the rhs. of eq. (5), is excluded here in order to focus on the effect of the coherent scattering length of the hydrogen atom. The prepeak is present in both PC-d_6 and PC-h_6 solutions, but it is not observed in PC-m_6 one. The prepeak of PC-h_6 solution is slightly shifted to the lower-q from that of PC-d_6 one. Although the characteristics above are in harmony with the experimental results in Fig. 1b, the strong low-q scattering in PC-m_6 solution is not reproduced in Fig. 4b.

The low-q scattering in PC-m_6 solution is ascribed to the intramolecular correlation, as is demonstrated in Fig. 4c. The intramolecular correlation exhibits a strong peak at q = 0, as is shown with the blue symbols. Combining the first and the second terms of the rhs. of eq. (5), the strong low-q scattering of $^7LiClO_4$ / PC-m_6 solution is reproduced, as is shown with the green symbols. It should be stressed again here that the intramolecular correlation term, the rhs. of eq. (5), works solely in PC-m_6. It vanishes in PC-d_6 or PC-h_6 because x_H = 0 or x_D = 0, respectively. The presence of the q = 0 peak solely in PC-m_6 thus supports our assignment of the peak to the intramolecular correlation term, the rhs. of eq. (5). In summary, the MD simulation with Model 1 describes the essential feature of the isotope substitution effects of the prepeak structure of $LiClO_4$ / PC solution.

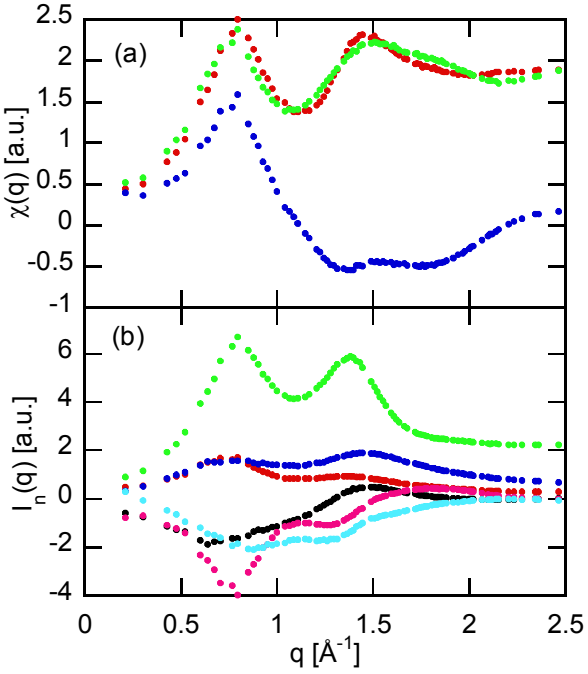

Figure 5. Partial structure factors of $^{7}LiClO_4$ / PC-d_6 solutions are plotted. Panel (a) shows the partial structure factors between Li-Li (red), Li-Cl (blue), and Cl-Cl (green) . In panel (b), the neutron static structure factors, $I_n(q)$s, are divided into the contributions of various domains, including ion-ion (red), PCpol-PCpol (blue), nonpol-nonpol (green), ion-PCpol (black), ion-nonpol (pink), and PCpol-nonpol (aqua) contributions.

The partial structure factors are analyzed hereafter in order to resolve the origin of the prepeak in detail. The partial structure factors associated with the cation and the anion are shown in Fig. 5a, where the Cl-atom is chosen as the center of the ClO_4^- anion.

The self correlations, the Li-Li and Cl-Cl components, exhibit strong peaks at the wavenumber of the prepeak. In addition, the strong *positive* cross correlation is observed there. The positive cross correlation indicates that the fluctuations of the number densities of the cation and the anion are in phase, and the prepeak is associated with the fluctuation of the ion concentration. The positive cross correlation between the positive and negative charges is a characteristic of the prepeaks of ionic liquids and higher alcohols,[15,19] which suggests that the prepeak of the concentrated $LiClO_4$ / PC solution possesses a similar origin to those of ionic liquids and higher alcohols.

The negative cross correlation between the two ions, which is a characteristic of the charge alternation mode,[15] is observed at the wavenumber of the main peak, q = 1.4 Å^{-1}. Therefore, the charge alternation mode belongs rather to the main peak.

The atoms in the system are categorized into three parts in Fig. 5b in order to divide the total structure factor of $^{7}LiClO_4$ / PC-d_6 into the contributions of the individual parts. The first part (ion) is composed of the cation and the anion. The second part (PCpol) is the polar part of the solvent PC, that is, -OCOO- group. The third one (nonpol) is the nonpolar part corresponding to the propylene group (-$CH_2CH(CH_3)$-) of PC.

The self correlation of these three parts exhibit positive peaks at the prepeak. On the other hand, all the cross correlations are negative there. In particular, the cross correlation between the ion and nonpol parts is strongly negative. Therefore, we can ascribe the prepeak to the contrast of the scattering length densities of the two domains composed of the ion and nonpol parts, respectively. Kaur and coworkers reported that the prepeak of deep eutectic solvents, that is, the concentrated solutions of $LiClO_4$ in alkylamides, accompanies the strong negative correlation between the salts and solvents.[22] Based on the negative correlation, they assigned the prepeak to the domain structure composed of ionic and solvent parts. The prepeak we observed in the $LiClO_4$ / PC solution thus possesses the similar origin to that of the deep eutectic solvents, and we suspect that the prepeak structure may be common to the concentrated solutions of lithium salts in amphiphilic solvents.

The effects of the isotope substitution on the strength of the prepeak can be realized based on the assignment above. The scattering length density of the nonpol domain is *higher* than that of the ion domain in $^{7}LiClO_4$ / PC-d_6 solution. The substitution of ^{7}Li with ^{6}Li increases the scattering length density of the ion domain, which results in the decrease in the contrast of the scattering length densities of the two domains.

The effect of the H / D substitution is more significant owing to both the large difference in b_H and b_D and the large number of the hydrogen atoms in PC. The scattering length density of the nonpol domain of $^{7}LiClO_4$ / PC-h_6 solution is now *lower* than that of the ion domain, and the prepeak appears reflecting

the difference in the scattering length densities of these two domains. At the intermediate degree of the H / D isotope substitution, however, the scattering length densities of the ion and nonpol domains become close to each other, which explains the disappearance of the prepeak in the case of $^{7}LiClO_4$ / PC-m_6 solution.

Given the similar origin of the prepeak of the concentrated lithium electrolytes with that of room-temperature ionic liquids, it is an interesting and important question how the prepeak structure affects the transport properties of the electrolytes such as ionic conductivity and shear viscosity. We have analyzed the dynamics of model ionic liquids based on the mode-coupling theory (MCT).[43] The analysis showed that there are two different mechanisms by which the prepeak structure increases the shear viscosity of ionic liquids. The first one is the direct coupling between the polarity density mode at the prepeak and the shear stress. The second one is the indirect coupling through the dynamics at the main peak. In the second mechanism, the microscopic dynamics of ions within the ionic domain is retarded due to the restriction of the domain structure. Since our previous experiment showed that the shear relaxation of the $LiPF_6$ / PC solution is explained by the intermediate scattering function at the main peak, the first direct mechanism is rather marginal. We consider that the second indirect mechanism works also in concentrated lithium electrolytes, which will be related to the rapid increase in the shear viscosity with increasing the salt concentration.

5. Conclusion

The structure of the concentrated $LiClO_4$ / PC solution was investigated by means of NDIS experiment and MD simulation. The variation of the height of the prepeak experimentally observed was reproduced by MD simulation. The MD simulation demonstrated that the prepeak was ascribed to the chain-like structure of ions, and the variation of the peak height was explained in terms of the contrast of the scattering length densities between the ionic and nonpolar domains.

Acknowledgments

The neutron diffraction experiment was performed under the general user program of Materials and Life Science Experimental Facility, Japan Proton Accelerator Research Complex (MLF, J-PARC) with the project number of 2015A0062. Tsuyoshi Yamaguchi was partly supported by the Japan Society for the Promotion of Science (JSPS), KAKENHI Grant No. 16K05514, and Yasuo Kameda was supported partly by JSPS, KAKENHI Grant No. 26391001.

Supporting Information

The Supporting Information is available free of charge via the Internet at http://pubs.acs.org/.

The calibration method of the effects of inelastic scattering on the structural analysis using the total diffractometer NOVA in MLF, J-PARC, the temperature dependence of the structure factor $I_n(q)$ of $^7LiClO_4$ / PC-d_6 calculated by MD simulation using Model 1, and the solvation structures of Li^+ atom determined by MD simulation with different models.

REFERENCES

(1) Yoshida, K.; Nakamura, M.; Kazue, Y.; Tachikawa, N.; Tsuzuki, S.; Seki, S.; Dokko, K.; Watanabe, M. Oxidative-Stability Enhancement and Charge Transport Mechanism in Glyme-Lithium Salt Equimolar Complexes. *J. Am. Chem. Soc.* **2011**, *133*, 13121–13129.

(2) Yamada, Y.; Furukawa, K.; Sodeyama, K.; Kikuchi, K.; Yaegashi, M.; Tateyama, Y.; Yamada, A. Unusual Stability of Acetonitrile-Based Superconcentrated Electrolytes for Fast-Charging Lithium-Ion Batteries. *J. Am. Chem. Soc.* **2014**, *136*, 5039–5046.

(3) Suo, L.; Borodin, O.; Gao, T.; Olguin, M.; Ho, J.; Fan, X.; Luo, C.; Wang, C.; Xu, K. "Water-in-Salt" Electrolyte Enables High-Voltage Aqueous Lithium-Ion Chemistries. *Science* **2015**, *350*, 938–943.

(4) Zhang, Q.; Vigier, K. D. O.; Royer, S.; Jérôme, F. Deep Eutectic Solvents: Syntheses, Properties and Applications. *Chem. Soc. Rev.* **2012**, *41*, 7108–7146.

(5) Smith, E. L.; Abbott, A. P.; Ryder, K. S. Deep Eutectic Solvents (DESs) and Their Applications. *Chem. Rev.* **2014**, *114*, 11060–11082.

(6) Alonso, D. A.; Baeza, A.; Chinchilla, R.; Guillena, G.; Pastor, I. M.; Ramón, D. J. Deep Eutectic Solvents: The Organic Reaction Medium of the Century. *Euro. J. Org. Chem.* **2016**, *4*, 612–632.

(7) Kameda, Y.; Suzuki, S.; Ebata, H.; Usuki, T.; Uemura, O. The Short-Range Structure around Li^+ in Highly Concentrated Aqueous LiBr Solutions. *Bull. Chem. Soc. Jpn.* **1997**, *70*, 47–53.

(8) Kameda, Y.; Umebayashi, Y.; Takeuchi, M.; Wahab, M. A.; Fukuda, S.; Ishiguro, S.; Sasaki, M.; Amo, Y.; Usuki, T. Solvation Structure of Li^+ in Concentrated $LiPF_6$-Propylene Carbonate Solutions. *J. Phys. Chem. B* **2007**, *111*, 6104–6109.

(9) Saito, S.; Watanabe, H.; Hayashi, Y.; Matsugami, M.; Tsuzuki, S.; Seki, S.; Lopes, J. N. C.; Atkin, R.; Ueno, K.; Dokko, K.; Watanabe, M.; Kameda, Y.; Umebayashi, Y. Li+ Local Structure in Li-Tetraglyme Solvate Ionic Liquid Revealed by Neutron Total Scattering Experiments with the $^{6/7}$Li Isotopic Substitution Technique. *J. Phys. Chem. Lett.* **2016**, *7*, 2832–2837.

(10) Mei, Q.; Benmore, C. J.; Sen, S.; Sharma, R.; Yarger, J. L. Intermediate Range Order in Vitreous Silica from a Partial Structure Factor Analysis. *Phys. Rev. B* **2008**, *78*, 144204.

(11) Lopes, J. N. A. C.; Pádua, A. A. H. Nanostructural Organization in Ionic Liquids. *J. Phys. Chem. B* **2006**, *110*, 3330–3335.

(12) Russina, O.; Triolo, A. New Experimental Evidence Supporting the Mesoscopic Segregation Model in Room Temperature Ionic Liquids. *Faraday Discuss.* **2012**, *154*, 97–109.

(13) Fujii, K.; Kanzaki, R.; Takamuku, T.; Kameda, Y.; Kohara, S.; Kanakubo, M.; Shibayama, M.; Ishiguro, S.; Umebayashi, Y. Experimental Evidences for Molecular Origin of Low-Q Peak in Neutron/X-Ray Scattering of 1-Alkyl-3-methylimidazolium Bis(trifluoromethanesulfonyl)amide Ionic Liquids. *J. Chem. Phys.* **2011**, *135*, 244502.

(14) Shimizu, K.; Bernardes, C. E. S.; Lopes, J. N. C. Structure and Aggregation in the 1−Alkyl-3-Methylimidazolium Bis(trifluoromethylsulfonyl)imide Ionic Liquid Homologous Series. *J. Phys. Chem. B* **2014**, *118*, 567–576.

(15) Kashyap, H. K.; Hettige, J. J.; Annapureddy, H. V. R.; Margulis, C. J. SAXS Anti-Peaks Reveal the Length-Scales of Dual Positive–Negative and Polar–Apolar Ordering in Room-Temperature Ionic Liquids. *Chem. Commun.* **2012**, *48*, 5103–5105.

(16) Tomšič, M.; Bešter-Rogač, M.; Jamnik, A.; Kunz, W.; Touraud, D.; Bergmann, A.; Glatter, O.; Nonionic Surfactant Brij 35 in Water and in Various Simple Alcohols: Structural Investigations by Small-Angle X-Ray Scattering and Dynamic Light Scattering. *J. Phys. Chem. B* **2004**, *108*, 7021–7032.

(17) Tomšič, M.; Jamnik, A.; Fritz-Popovski, G.; Glatter, O.; Vlček, L. Structural Properties of Pure Simple Alcohols from Ethanol, Propanol, Butanol, Pentanol, to Hexanol: Comparing Monte-Carlo Simulations with Experimental SAXS Data. *J. Phys. Chem. B* **2007**, *111*, 1738–1751.

(18) Böhmer, R.; Gainaru, C.; Richert, R. Structure and Dynamics of Monohydroxy Alcohols - Milestones Towards Their Microscopic Understanding, 100 Years after Debye. *Phys. Rep.* **2014**, *545*, 125–195.

(19) Perera, A. Charge Ordering and Scattering Pre-peaks in Ionic Liquids and Alcohols. *Phys. Chem. Chem. Phys.* **2017**, *19*, 1062–1073.

(20) Aguilera, L.; Xiong, S.; Scheers, J.; Matic, A. A Structural Study of LiTFSI-tetraglyme Mixtures: From Diluted Solutions to Solvated Ionic Liquids. *J. Mol. Liq.* **2015**, *210B*, 243–251.

(21) Shimizu, K.; Freitas, A. A.; Atkin, R.; Warr, G. G.; FitzGerald, P. A.; Doi, H.; Saito, S.; Ueno, K.; Umebayashi, Y.; Watanabe, M. et al. Structural and Aggregate Analyses of (Li Salt + Glyme) Mixtures; the Complex Nature of Solvate Ionic Liquids. *Phys. Chem. Chem. Phys.* **2015**, *17*, 22321–22335.

(22) Kaur, S.; Gupta, A.; Kashyap, H. K. Nanoscale Spatial Heterogeneity in Deep Eutectic Solvents. *J. Phys. Chem. B* **2016**, *120*, 6712–6720.

(23) Yamaguchi, T.; Yonezawa, T.; Yoshida, K.; Yamaguchi, T.; Nagao, M.; Faraone, A.; Seki, S. Relationship between Structural Relaxation, Shear Viscosity, and Ionic Conduction of $LiPF_6$/Propylene Carbonate Solutions. *J. Phys. Chem. B* **2015**, *119*, 15675–15682.

(24) Hansen, J.-P.; McDonald, I. R. *Theory of Simple Liquids*, 2nd ed.; Academic Press; London, 1986.

(25) NCNR, NIST Center for Neutron Research (2013), https://www.ncnr.nist.gov/resources/n-lengths/ (accessed 2017-01-06).

(26) Cotton, J. P. Small Angle Scattering and Polymers; In Introduction to Neutron Scattering, Lecture Notes of the Introductory Course 1st European Conference on Neutron Scattering (ECNS '96), Interlaken, Switzerland, October 6-11, 1996; Furrer A. Ed.; Paul Scherrer Institut: Villigen, 1996; pp. 144-161. http://www.iaea.org/inis/collection/NCLCollectionStore/_Public/28/024/28024527.pdf (accessed 2017-03-01).

(27) Paaiman, H. H.; Pings, C. J. Numerical Evaluation of X-Ray Absorption Factors for Cylindrical Samples and Annular Sample Cells. *J. Appl. Phys.* **1962**, *33*, 2635–2639.

(28) Soper, A. K.; Egelstalf, P. A. Multiple Scattering and Attenuation of Neutrons in Concentric Cylinders: I. Isotropic First Scattering. *Nucl. Instrum. Methods* **1980**, *178*, 415–425.

(29) NOVA Project, Analysis of Ordered/Disordered Structure in Hydrides with Total Scattering Technique (2015), http://research.kek.jp/group/hydrogen/analysis.html (accessed 2017-01-06).

(30) Placzek, G. The Scattering of Neutrons by Systems of Heavy Nuclei. *Phys. Rev.* **1952**, *86*, 377–388.

(31) Kameda, Y.; Sasaki, M.; Usuki, T.; Otomo, T.; Itoh, K.; Suzuya, K.; Fukunaga, T. Inelasticity Effect on Neutron Scattering Intensities of the Null-H_2O. *J. Neutron Res.* **2003**, *11*, 153−163.

(32) You, X.; Chaudhari, M. I.; Rempi, S. B.; Pratt, L. R. Dielectric Relaxation of Ethylene Carbonate and Propylene Carbonate from Molecular Dynamics Simulations. *J. Phys. Chem. B* **2016**, *120*, 1849–1853.

(33) Soetens, J.-C.; Millot, C.; Maigret, B. Molecular Dynamics Simulation of $Li^+BF_4^-$ in Ethylene Carbonate, Propylene Carbonate, and Dimethyl Carbonate Solvents. *J. Phys. Chem. A* **1998**, *102*, 1055–1061.

(34) Heinje, G.; Luck, W. A. P.; Heinzinger, K. Molecular Dynamics Simulation of an Aqueous $NaClO_4$ Solution. *J. Phys. Chem*. **1987**, *91*, 331–328.

(35) Cadena, C.; Maginn, E. J. Molecular Simulation Study of Some Thermophysical and Transport Properties of Triazolium-Based Ionic Liquids. *J. Phys. Chem. B* **2006**, *110*, 18026–18039.

(36) Kasahara, K.; Sato H. Development of three-dimensional site-site Smoluchowski-Vlasov equation and application to electrolyte solutions. *J. Chem. Phys*. **2014**, *140*, 244110.

(37) Jensen, K. P.; Jorgensen, W. L. Halide, Ammonium, and Alkali Metal Ion Parameters for Modeling Aqueous Solutions. *J. Chem. Theory Comput.* **2006**, *2*, 1499–1509.

(38) Abraham, M. J.; Murtola, T.; Schulz, R.; Pall, S.; Smith, J. C.; Hess, B.; Lindahl, E. GROMACS: High Performance Molecular Simulations through Multi-Level Parallelism from Laptops to Supercomputers. *SoftwareX* **2015**, *1*, 19–25.

(39) Allen, M. P.; Tildesley, D. J. *Computer Simulation of Liquids*; Clarendon Press; Oxford, 1987.

(40) Hess, B.; Bekker, H.; Berendsen, H. J. C.; Fraaije, J. G. E. M. LINCS: A Linear Constraint Solver for Molecular Simulations. *J. Comp. Chem.* **1997**, *18*, 1463–1472.

(41) Humphrey, W.; Dalke, A.; Schulten, K. VMD - Visual Molecular Dynamics. *J. Molec. Graphics* **1996**, *14*, 33–38. http://www.ks.uiuc.edu/Research/vmd/ (accessed March, 2016).

(42) Seo, D. M.; Afroz, T.; Allen, J. L.; Boyle, P. D.; Trulove, P. C.; De Long, H. C.; Henderson, W. A. Structural Interactions within Lithium Salt Solvates: Cyclic Carbonates and Esters. *J. Phys. Chem. C* **2014**, *118*, 25884–25889.

(43) Yamaguchi T. Mode-Coupling Theoretical Study on the Roles of Heterogeneous Structure in Rheology of Ionic Liquids. *J. Chem. Phys.* **2016**, *144*, 124514.

TOC Graphic: